Quantitative Analysis of the Tomographic Thallium-201 Myocardial Bullseye Display: Critical Role of Correcting for Patient Motion

Robert Eisner, André Churchwell, Till Noever, Dave Nowak, Karen Cloninger, Daniel Dunn, Wilma Carlson, Joel Oates, Janie Jones, Douglas Morris, Henry Liberman, and Randolph Patterson

Carlyle Fraser Heart Center of Emory University at Crawford W. Long Memorial Hospital, Department of Medicine, Department of Radiology, Emory University School of Medicine, Atlanta, Georgia; and General Electric Medical Systems Group, Milwaukee, Wisconsin

Single photon emission computed tomography (SPECT) myocardial ^{201}Tl imaging appears to offer major improvements over planar imaging. Quantitative analysis of the ^{201}Tl images appears to offer major advantages over subjective analysis in planar imaging, but the three-dimensional data available in SPECT images requires special approaches to analysis and display. Thus the myocardial "bullseye" display was developed to summarize and analyze the three-dimensional images of the left ventricle in two dimensions. The relative ^{201}Tl distribution to each region of the left ventricle of an individual patient can be displayed as the number of s.d.s away from normal that the region falls. We found that patient motion during the 22 min required for SPECT imaging appeared to produce artifactual defects. Thus, computer programs were developed to quantitate motion between consecutive frames of a [^{201}Tl] SPECT myocardial imaging study, simulate nonreturning vertical motion in normal patients, and correct the acquired data for motion. Motion as small as 0.5–1.0 pixel (3–6 mm) in the vertical (axial) direction caused artifactual defects in the quantitative bullseye display that resulted in a false-positive rate of up to 40% for a +1.0 pixel shift. Patient motion of magnitude greater than the threshold value for artifact-production (0.5 pixel) occurred at a rate of 10%, and should be corrected before tomographic reconstruction.

J Nucl Med 29:91–97, 1988

Quantitative single photon emission computed tomographic (SPECT) thallium-201 (^{201}Tl) myocardial imaging has been reported (*1–3*) to be a sensitive and specific test for the diagnosis of coronary artery disease. However, the studies reported have been those where quality control procedures indicated no particular problem with the acquired data. Quality control of the camera/gantry and computer processing parameters required to produce an accurate ^{201}Tl tomogram have been previously described (*4–7*). It must be emphasized, however, that acquisition of a ^{201}Tl tomographic scan requires 20–25 min, during which time the patient must lie still under the camera immediately after a high level of exercise. We had noted artifactual defects in the data of some patients who had shown gross movement. This paper discusses the establishment of a threshold for the amount of motion above which artifactual defects were produced, and the determination of the extent and frequency of motion in ^{201}Tl scans above this value. To avoid subjecting the patient to a second exercise test, with the associated risks and inconvenience, a correction program was developed for use on scans in which excessive motion occurred.

Received Dec. 23, 1986; revision accepted July 8, 1987.

For reprints contact: R. L. Eisner, PhD, Director, Imaging Science Laboratory, Dept. of Radiology, Emory University School of Medicine, 412 Woodruff Memorial Building, Atlanta, GA 30322.

METHODS

Tomographic Acquisition Parameters

Within 5 min of injection of 3.5 mCi ^{201}Tl at peak stress tomographic image acquisition was started. Delayed imaging followed ~3 to 4 hr later. For each study, the tomographic data were obtained from a 32-view, 40 sec/stop, 180° anterior arc scan using a 45° right anterior oblique starting position. At each view, data were acquired into a 64 × 64 digital matrix with each pixel in the array having a linear dimension of ~6

mm. The planar views were uniformity corrected using correction factors obtained from a 30 million count cobalt-57 flood acquisition.

Summary of Bullseye Quantitative Program

To improve the signal to noise ratio, the raw view data were nine-point smoothed using a

$$\begin{matrix} 1 & 2 & 1 \\ 2 & 4 & 2 \\ 1 & 2 & 1 \end{matrix}$$

convolution kernel. One-pixel-thick transaxial slices were reconstructed using a conventional Ramp-filtered backprojection algorithm. An oblique angle slice reconstruction routine reoriented the transaxial slices along the three mutually perpendicular planes (i.e., horizontal and vertical long axis and short axis) in a coordinate system fixed to the heart. From apex to base, each of the short axis slices was subjected to a circumferential profile analysis. Maximum count profiles were extracted along each of 40 radial vectors drawn at 9° angular intervals from the center of the heart. These intensity profiles were displayed in a color-coded polar map. Displays of this map have the center corresponding to the apex, and the periphery to the basal region. As shown in Figure 1A, the "bullseye" display format gives quantitative information about the ^{201}Tl uptake in each wall of the myocardium.

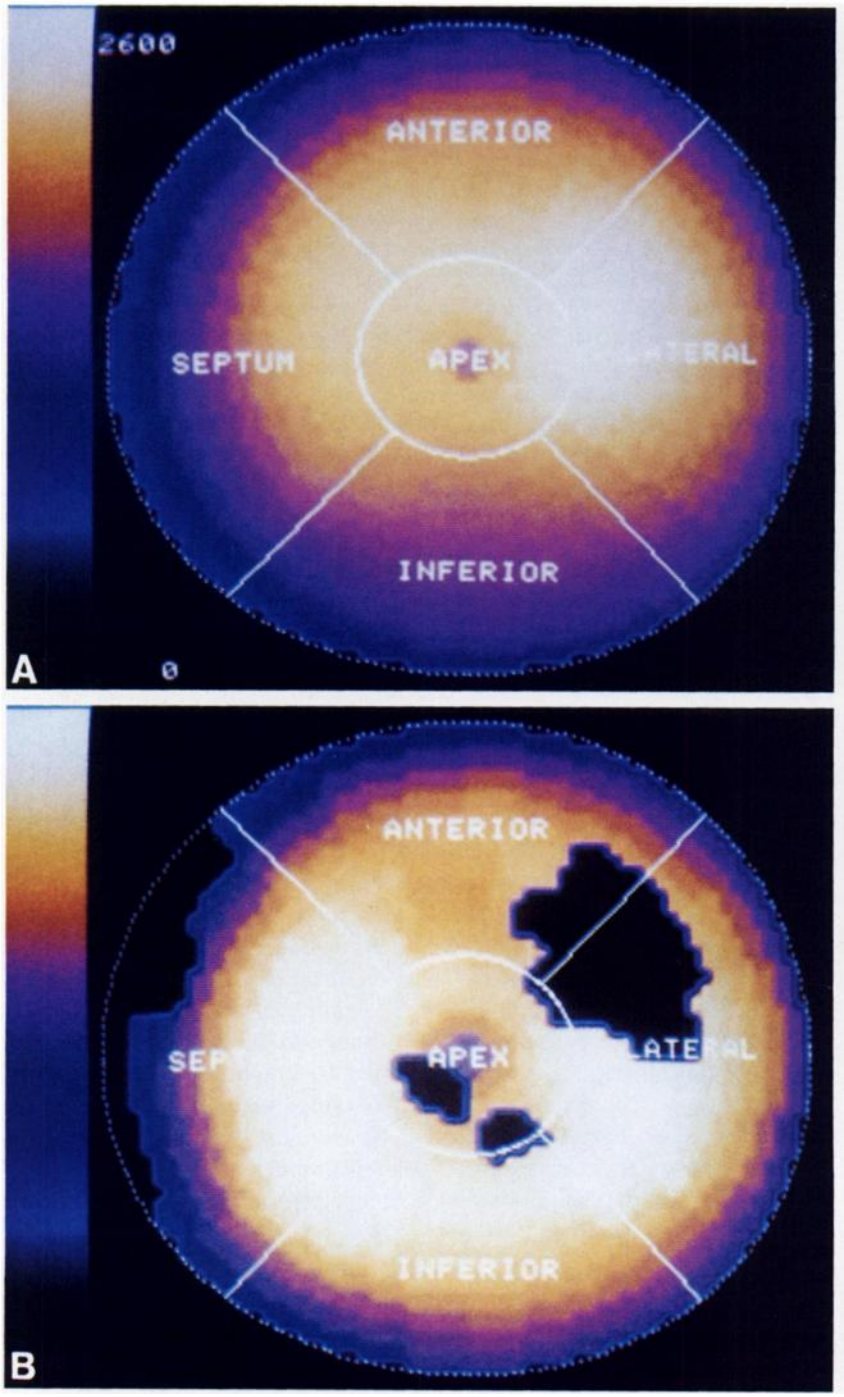

FIGURE 1
A: Quantitative ^{201}Tl bullseye display. B: Bullseye display showing blackened pixels for data that deviate by more than 2.5 s.d. from the matched normal file.

Separate normal files were obtained from male and female subjects who had <5% probability (*8–9*) of coronary artery disease (low probability of disease (LPD). A patient's bullseye image was compared to its matched normal-file, and the number of s.d.s below normal was obtained for each pixel. Pixels that deviated by more than 2.5 s.d.s from normal were blackened on the bullseye display (Fig. 1B).

Vertical Motion Quantitation and Correction Technique

The motion quantitation and correction technique is based upon a cross-correlation algorithm (*10*), that was developed to detect patient motion during a tomographic scan. Here, we use the algorithm to analyze only sudden and vertical (axial) motion: for each view, n, of the tomographic study the summed counts along the horizontal direction, Pn(j), were obtained for each of the 64 pixels, j, in the vertical direction. The cross-correlation functions, CCn(s), were calculated between consecutive views n-1 and n of the tomographic study:

$$CCn(s) = \sum_{j=1}^{64} Pn(j)*Pn - 1(j + s) \qquad (1)$$

for integer values of the variables, s, between −10 and 10. The maximum value of the cross-correlation functions, CCn (smax), occurs at the value s = smax.

The correlation-determined shift between adjacent frames of the tomographic scan was extracted from a parabolic fit to CCn (smax) and its two neighboring points, CCn (smax − 1) and CCn (smax + 1). An example of the distribution derived from cross-correlation fits to data taken after physically moving the scanning table on which the patient rested just before the acquisition of frame 16 (see below) is shown in Figure 2A (solid curve). The deviation, in frame 16, below the smoothly varying frame-to-frame background indicates that motion occurred. As discussed elsewhere (*10*), the background component derives from non-motion-induced effects, such as attenuation, that vary over the course of the acquisition, and that we described by a second order polynomial in view angle. The presence of the background component precludes analysis of gradual vertical motion during acquisition. The coefficients of the polynomial were obtained from a least-squares fit to the data. The dashed curve in Figure 2A resulted from the polynomial fit to the solid curve in the figure. The individual frame motion components (Figure 2B) were extracted from data obtained from subtraction of the fitted curve from the original curve subject to the constraint that its magnitude was larger than a predefined lower limit. Based upon the discussion below, we have chosen this value as 0.5 pixel, the threshold for motion-induced, false-positive clinical results. With this constraint, the only significant motion component in Figure 2B, is between frame 15 and frame 16 (0.8 pixel). No other pixel-shift values are above the threshold, so that for this example, frame 16 and all subsequent frames would have to be "moved" by 0.8 pixel to correct for patient "motion". In the more general case, in which the patient moved many times over the course of the scan, the total motion-component for a particular frame (with respect to frame one) is obtained by summing all the individual motion components obtained from all preceding frames. A frame is motion-corrected by shifting of the original frame data in the vertical direction by this amount. For non-integral shift values, the motion-corrected frame is obtained by linear interpolation of the vertical rows in the unshifted original digital frame data.

Patient Data

To test for the effect of motion on diagnostic accuracy required that the amount of patient motion be controlled over a large range. This was a task not easily accomplished with real subjects. The alternative we employed was to computer-simulate motion in stress tomographic data from five female and five male subjects with low probability of disease in whose data no motion was apparent. Absence of motion was determined by inspecting a rotating cine display of the view data, and by evaluating the output from the quantitative cross-correlation detection algorithm. Simulation of nonreturning patient movement was accomplished by arbitrarily "translating" the data by a given number of pixels for a particular view and all subsequent frames. As shown below, the time at which a patient was likely to move showed no correlation with the

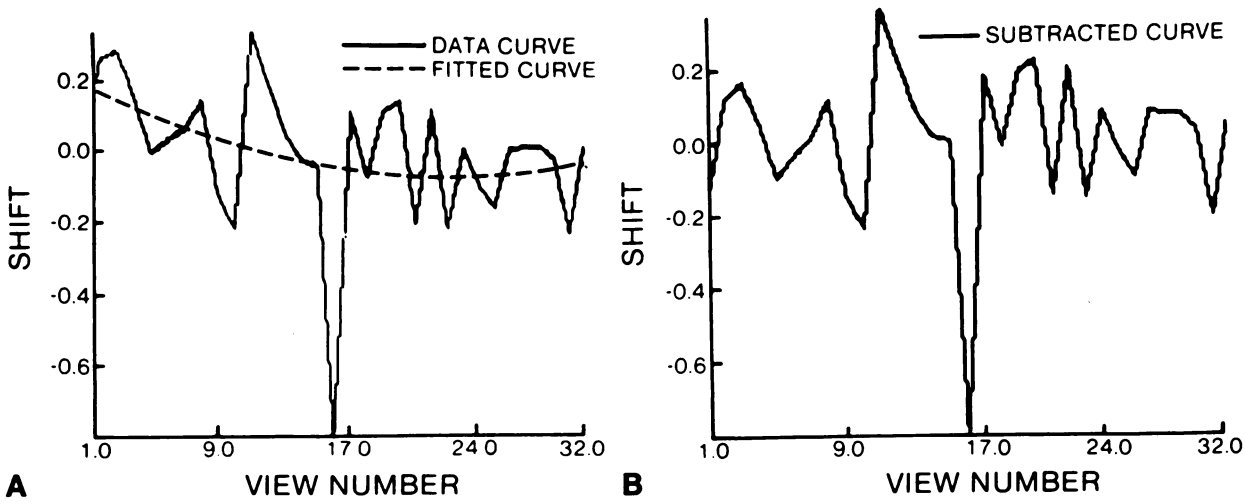

FIGURE 2

A: Frame-to-frame pixel shifts (solid curve) determined from a ^{201}Tl study in which the table was moved by 0.9 pixel before the acquisition of frame 16. The dotted curve is the result of a fit with a second order polynomial. B: Curve formed by taking the difference between the two curves shown in Fig. 2A. The 0.8 pixel component of motion, between frame 15 and 16, is extracted from the curve.

TABLE 1
Accuracy of Motion-Detection Algorithm

Type of motion	Input (pixels)	Extracted (pixels)
Simulated-returning	0.7	0.74 ± 0.08
Simulated-nonreturning	0.7	0.68 ± 0.08
Simulated-returning	−0.7	−0.68 ± 0.08
Simulated-nonreturning	−0.7	−0.64 ± 0.08
Table movement	0.9	0.8

tomographic study view number. We therefore chose frame 16 of the 32-view ^{201}Tl tomographic acquisition as the view in which to begin motion-simulation. The amount of simulated motion was varied between ±0.5 and ±3.0 pixel. After "computer-movement" the data were processed through the same tomographic reconstruction program used for clinical imaging. Following the procedure described above, tomographic slices were passed through the quantitative bullseye program.

To test the accuracy of the motion algorithm, simulated returning (i.e., patient moved in frame 16 and returned to the same position in frame 17) and nonreturning motion (i.e., the more likely case in which the patient moved and did not move back to the original position) were simulated. Based on the range of patient motion we observed, we chose to shift the stress data of the ten LPD patients by ±0.7 pixels. Additional data were acquired to test the accuracy of the motion correction technique. Following acquisition of the stress scan, a second study was performed in which the scanning table upon which the subject rested was moved by a known calibrated distance (0.9 pixel) before the acquisition of frame 16 of the tomographic scan.

To quantitate the frequency and extent of patient motion, stress tomographic ^{201}Tl data from 100 randomly selected patients were processed through the motion-detection algorithm. Those data which showed a significant motion component were motion-corrected and passed through the reconstruction and bullseye quantitative program. Results were compared with the uncorrected data as well as with those obtained from cardiac angiography.

RESULTS

Accuracy of the Motion Detection Algorithm

Table 1 shows the average and s.d. of the extracted motion-component from the motion-simulated stress studies of the ten subjects with low probability of disease. There is an excellent agreement between the extracted and input values. Also shown in Table 1 is that there is good agreement between the expected (0.9 pixel) and the extracted (0.8 pixel) value for the study in which the table was physically moved.

From these studies, and from our experience with the clinical use of the technique, we concluded that patient motion of magnitude sufficient to produce artifactual defects (i.e., 0.5 pixel) could easily be detected and corrected for.

View Independence of Patient Motion During Thallium-201 Tomographic Acquisition

Using the motion-detection algorithm, the view corresponding to the maximum extracted pixel movement was obtained from each of the 100 tomographic stress acquisitions. The distribution (Fig. 3) shows that patient movement can occur at any time (i.e., view) during the tomographic acquisition.

Effect Of Nonreturning Vertical Motion on Tomographic Data from Normal Subjects

Two observers noted no significant defects in bullseye displays obtained from the unshifted reconstructed images of the ten (low probability of disease) subjects. The results of the readings associated with the motion-

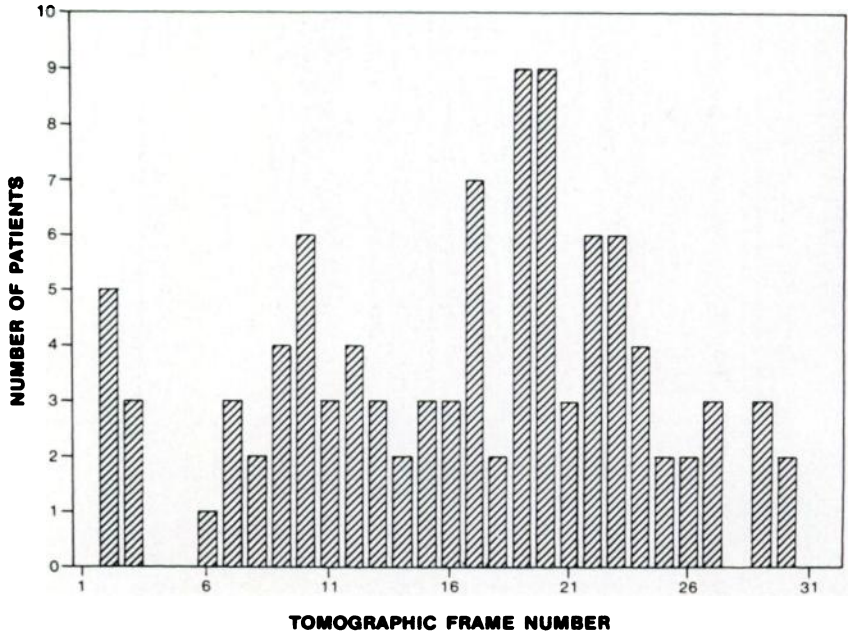

FIGURE 3
For the 100 randomly selected patients a histogram is shown of the view corresponding to the maximum extracted motion component in the stress study.

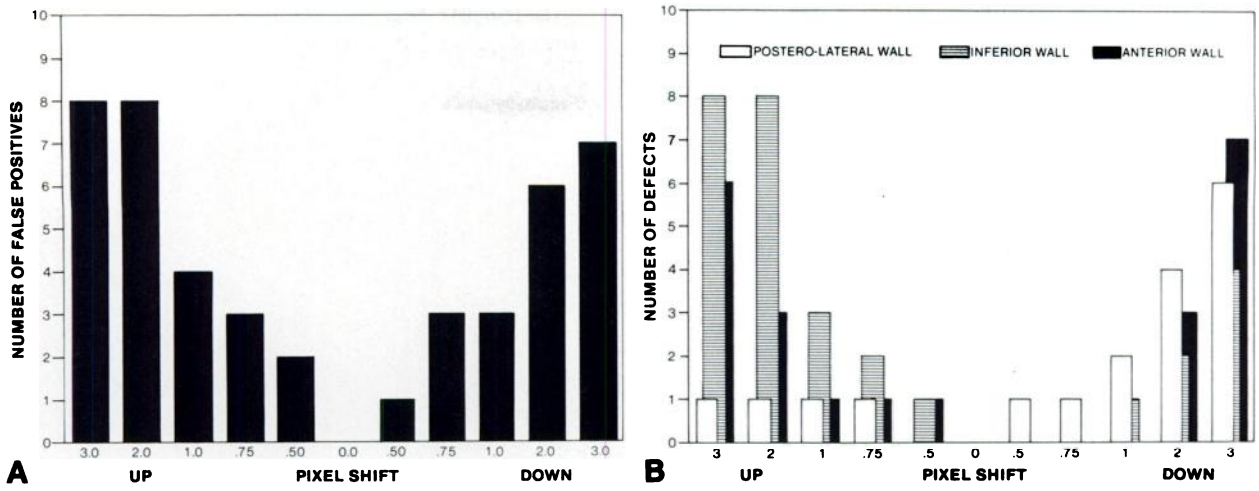

FIGURE 4
A: For n = 10, the number of false-positive results is shown for various simulated pixel shifts. B: For n = 10, the position of the defect on the bullseye display is shown for various simulated pixel shifts.

simulated studies are summarized in Figure 4A, where the number of false-positive readings is given for each of ten induced pixel shifts. These data show that for pixel shifts as small as 0.5–1.0 pixel significant artifactual defects appear, and lead to a false-positive rate of up to 40% at +1.0 pixel.

As shown in Figure 4B, the location of the defects in the myocardial wall depended on the direction of the shift. Upward shifts primarily caused inferior wall defects and downward shifts posterolateral wall defects. Figures 5A and 5B show two examples of bullseye displays in which motion-induced artifactual defects are apparent. The corresponding bullseye displays obtained from the original unshifted data, Figures 5C and 5D, do not exhibit these defects.

Frequency and Extent of Motion in Patient Acquisitions

The frequency of motion with an amplitude of greater than the artifact-threshold value of 0.5 pixel was obtained from the output of the cross-correlation algorithm applied to the acquisition view data from the stress studies of the 100 randomly selected subjects. A histogram of the maximum motion component detected by the technique is shown in Figure 6. Ten percent (10/100) of the patients exhibited motion in

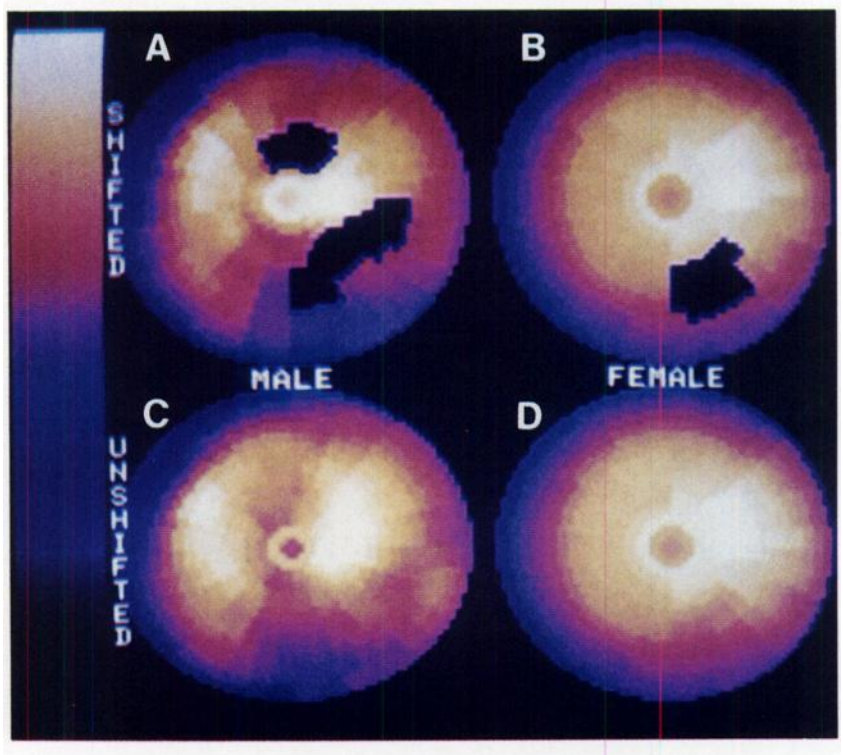

FIGURE 5
A: Bullseye display for a normal male subject following a simulated −0.75 shift of the data in the vertical direction in view 16 and all subsequent frames. B: Bullseye display for a normal female subject, but following a simulated +.75 shift of the data in the vertical direction in view 16 and all subsequent frames. C: Bullseye display of the original unshifted data for the normal male subject. D: Bullseye display of the original unshifted data for the normal female subject.

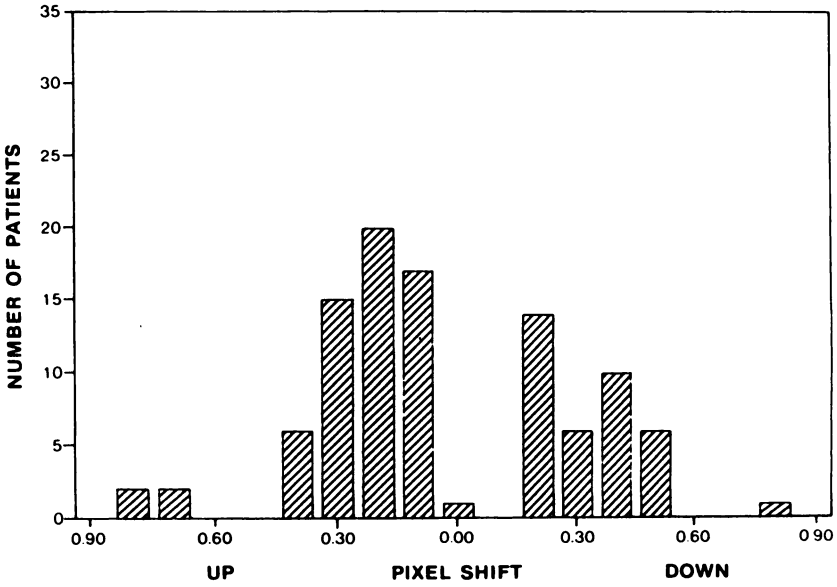

FIGURE 6
For the 100 randomly selected stress studies a histogram is shown of the maximum pixel shift extracted by the motion-detection program. Ten percent (10/100) exhibited motion >0.5 pixel.

their stress studies with a magnitude >0.5 pixel. In the seven patients with catheterization results, motion-correction clarified one false-positive and one false-negative result in the uncorrected data (Fig. 7-bullseye displays).

DISCUSSION

We have found that some patients have difficulty lying still for the duration of the tomographic scan. Initially, we observed apparently artifactual defects in two patients who had shown gross movement under the camera. Therefore, it seemed important to test for the effects of patient motion on tomographic ^{201}Tl imaging.

The investigation was limited to the effects caused by simple translational motion in the vertical direction. Although combinations of rotation and translation are easily detected, it is not possible, without some model

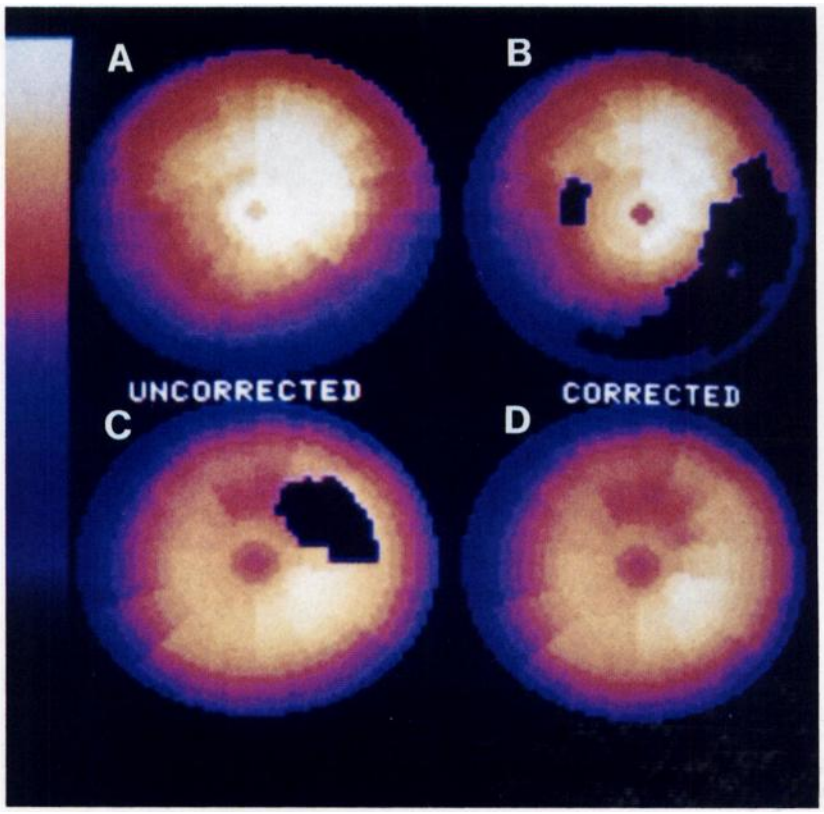

FIGURE 7
A: Bullseye display for a patient with motion corresponding to 0.9 pixel which occurred in frame 9 of the [^{201}Tl]SPECT study. The reading of this image was falsely negative. B: Following motion-correction of the data used in Figure 7A, the image was read as an infero-lateral wall defect. The patient had significant right coronary disease. C: Bullseye display for a patient with motion corresponding to 0.8 pixel which occurred in frame 11 of the [^{201}Tl]SPECT study. The reading of this image was falsely positive. D: Following motion-correction of the data used in Figure 7C, the image was read as a normal study. The patient had no significant coronary disease on coronary angiography.

of such motion to establish an exact relationship between the degree of motion and reconstructed image accuracy. Addition of other types of motion is expected to produce additional artifacts in the reconstructed images. Computer-simulated vertical motion appears to reproduce a frequently observed pattern of patient movement associated with stretching of the arms, shoulders, and thorax while on the scanning table.

The motion correction program uses the cross-correlation between summed vertical profiles from adjacent views of the tomographic study. In order for this approach to extract successfully the motion-component an adequate signal-to-background ratio from those objects that moved between frames was required. We found in some delayed scans with relatively large background that the algorithm tended to underestimate the degree of motion. Failure of the approach was indicated by the presence of residual motion in the rotating cine display of the corrected frame data. In such cases, improvement resulted when a constant background level was subtracted from each frame of the tomographic study.

The linear interpolation technique used to correct for motion results in motion-corrected frames which are smoothed in the vertical direction. This implies that the output from the computer-correction of motion is not completely equivalent to what would have been expected had the patient not moved at all. In order to understand why the correction procedure is nevertheless valid we note that during the reconstruction process, each frame of the ^{201}Tl data is smoothed. Additional smoothing takes place in the interpolation algorithm used to form the short axis slices, as well as in the algorithm that generates the bullseye display. Such a large degree of smoothing suggests that the smoothing due to the motion correction algorithm should result in little, if any, quantitative difference between reconstructed data from a motion-corrected acquisition and one that exhibited no patient motion. Furthermore, the improvement in accuracy of ^{201}Tl tomography following motion-correction is demonstrated by clarification of one false-positive and one false-negative without creating any incorrect results in the seven patients whose scans had a motion component of >0.5 pixel.

CONCLUSION

Care should be exercised when interpreting SPECT ^{201}Tl data when significant motion occurs. Patient motion in the vertical direction with a magnitude of >0.5 pixel (3.0 mm) is common (10/100), and can cause false-negative and false-positive readings (40% with +1.0 pixel (6.0 mm) shift). The false-positive rate was obtained for simulated nonreturning motion beginning with frame 16 of a 32-view tomographic ^{201}Tl study. The false-positive rate should be smaller for corresponding nonreturning patient motion beginning in frames other than the middle frame (i.e., frame 16) of the SPECT study. While we have only modeled simple vertical-translational motion, it is to be expected that the extent of artifactual defects and distortions are greater in data with additional translational and/or rotational motion. As a general quality control procedure we suggest that data that exhibit large pixel shifts (>0.5 pixel) in the vertical direction, should be motion-corrected before tomographic (SPECT) reconstruction is performed.

NOTE

* (General Electric 400 ACT/STAR) General Electric, Milwaukee, WI.

REFERENCES

1. Ritchie J, Williams DL, Harp G, et al. Transaxial tomography with thallium-201 for detecting remote myocardial infarction—comparison with planar imaging. *Am J Cardiol* 1982; 50:1236–1241.
2. Larsson SA. Gamma camera emission tomography. *Acta Radiologica Suppl* 1980; 363.
3. Garcia EV, Vantrain K, Maddahi J, et al. Quantification of rotational thallium-201 myocardial tomography. *J Nucl Med* 1985; 26:17–26.
4. Williams DL, Ritchie JL, Harp GD, et al. Preliminary characterization of the properties of a transaxial whole-body single-photon tomograph: emphasis on future application to cardiac imaging. In: Esser PD, ed. Functional mapping of organ systems and other computer topics. New York: Society of Nuclear Medicine, 1981:167–183.
5. Tamaki N, Mukai T, Ishii Y, et al. Comparative study of thallium emission myocardial tomography with 180° and 360° data collection. *J Nucl Med* 1982; 23:661–666.
6. Eisner RL, Nowak DJ, Pettigrew RI, et al. Fundamentals of 180° acquisition and reconstruction in SPECT imaging. *J Nucl Med* 1986; 11:1717–1728.
7. Tamaki N, Yonekuna Y, Mukai T. Stress thallium-201 transaxial emission computed tomography: quantitative versus qualitative analysis for evaluation of coronary artery disease. *J Am Coll Cardiol* 1984; 4:1213–1221.
8. Diamond GA, Forrester JS. Analysis of probability as an aid in the clinical diagnosis. *N Engl J Med* 1979; 300:1350–1358.
9. Patterson RE, Eng C, Horowitz SF. Practical diagnosis of coronary artery disease: a Bayes' theorem nomogram to correlate clinical data with noninvasive tests. *Am J Cardiol* 1984; 53:252–256.
10. Eisner RL, Noever T, Nowak DJ, et al. Use of cross-correlation to detect patient motion during SPECT imaging. *J Nucl Med* 1987; 28:57–101.